Journal of Power Sources 195 (2010) 6847–6853

Contents lists available at ScienceDirect

Journal of Power Sources

journal homepage: www.elsevier.com/locate/jpowsour

Effect of nano-silica filler in polymer electrolyte on Li dendrite formation in Li/poly(ethylene oxide)–$Li(CF_3SO_2)_2N$/Li

S. Liu[a,b], N. Imanishi[b,*], T. Zhang[b], A. Hirano[b], Y. Takeda[b], O. Yamamoto[b], J. Yang[a]

[a] School of Chemistry and Chemical Engineering, Shanghai Jiaotong University, Shanghai 200040, PR China
[b] Department of Chemistry, Faculty of Engineering, Mie University, Tsu 514-8507, Japan

ARTICLE INFO

Article history:
Received 2 February 2010
Received in revised form 8 April 2010
Accepted 8 April 2010
Available online 13 May 2010

Keywords:
Dendrite growth
Interfacial characteristic
Composite solid polymer electrolytes
Nano-SiO_2 filler

ABSTRACT

Lithium dendrite growth in Li/poly(ethylene oxide) (PEO)–$Li(CF_3SO_2)_2N$ (LiTFSI)–nano-SiO_2/Li was examined using direct *in situ* observation under galvanostatic conditions at 60 °C. Both the onset time of dendrite formation and the short-circuit time of the cells were extended by the addition of nano-SiO_2 filler into the polymer electrolyte, of which an acid-modified nano-SiO_2 filler was the most effective. The onset time was dependent on the current density in the range from 0.1 to 1.0 mA cm^{-2}. Li dendrite growth in Li/PEO_{18}LiTFSI/Li at 60 °C for current densities of 0.1 and 0.5 mA cm^{-2} started at 125 and 15 h, respectively. PEO_{18} LiTFSI with addition of 10 wt% acid-modified 50 nm SiO_2 showed extended dendrite formation onset times of 250 h at 0.1 mA cm^{-2} and 32 h at 0.5 mA cm^{-2}. The suppression of dendrite formation at the Li/PEO_{18} LiTFSI interface could be explained by enhancement of the conductivity and suppression of the interface resistance between lithium and the polymer electrolyte by addition of the nano-SiO_2 filler. The electrical conductivity of 4.1×10^{-4} S cm^{-1} and interface resistance of 405 Ω cm^2 for PEO_{18} LiTFSI at 60 °C were respectively increased to 7.2×10^{-4} S cm^{-1} and decreased to 77 Ω cm^2 by the addition of 10 wt% acid-modified nano-SiO_2.

1. Introduction

Increasing efforts have been devoted to the improvement of battery performance in order to develop high energy density batteries. Metallic lithium is a particularly good anode candidate for high energy density batteries, because it has a high theoretical specific capacity (3860 mAh g^{-1}) and high negative potential (−3.05 V vs. NHE). Nevertheless, the use of a metallic lithium anode is limited, due to the occurrence of dendrite growth during charging of the battery [1]. This phenomenon occurs even in polymer electrolytes, although to a lesser extent than in liquid electrolytes [2,3]. Dendrite formation is very detrimental to the operation of lithium batteries with respect to safety and battery life time [4].

Recently, lithium–air secondary batteries have been considered as the most attractive high specific energy battery for electric vehicles [5]. Their calculated energy density is as high as 11,140 Wh kg^{-1}, which is comparable to that of gasoline. The typical lithium–air battery consists of a lithium metal anode, a carbon air electrode, and a non-aqueous electrolyte. The lithium metal electrode is sensitive to water; therefore, protection of the lithium anode to corrosion by water from the air is a critical point for the application of lithium–air batteries. Water stable lithium metal electrodes have been proposed by Visco et al. [6] and by the current authors [7,8] that show prospective promise to solving the water corrosion problem of lithium metal. Our proposed water stable lithium electrode consists of lithium metal, a polymer electrolyte buffer layer of (poly(ethylene oxide) (PEO) with $Li(CF_3SO_2)_2N$ (LiTFSI)), and a water stable high lithium conducting glass ceramic layer of $Li_{1.35}Ti_{0.175}Al_{0.25}P_{2.7}Si_{0.3}O_{12}$. The polymer electrolyte interlayer serves to protect from the direct reaction of lithium metal and the solid electrolyte. The interface resistance of the three-layer lithium electrode is predominantly between the lithium metal and polymer electrolyte. However, for the application such lithium electrodes in high specific energy density lithium air batteries reduction of the Li/polymer electrolyte interface resistance as well as suppression of the lithium dendrite growth in the interface is required to obtain high power and energy density and a long cycle life. Short circuiting by dendrite formation in the Li/ethylene carbonate–ethyl methyl carbonate–dimethyl carbonate (1:1:1)–$LiPF_6$/Li cell was observed at 0.2 h during polarization under 1.0 mA cm^{-2} at 15 °C with a 1.0 mm thick separator [9]; the period until short circuit is too short. A gel-type polymer electrolyte comprised of 30 wt% PEO and poly(propylene oxide) (PPO) (5:1, w/w) copolymer and 70 wt% ethylene carbonate–propylene carbonate (1:1, w/w) showed improved suppression of dendrite formation, with dendrites appearing at 1 h under polarization at 0.8 mA cm^{-2} with a 1.0 mm thick separator [10]. In the case of a dry polymer electrolyte, a similar result with the gel-type polymer

* Corresponding author. Tel.: +81 59 231 9420; fax: +81 59 231 9478.
E-mail address: imanishi@chem.mie-u.ac.jp (N. Imanishi).

0378-7753/$ – see front matter © 2010 Elsevier B.V. All rights reserved.
doi:10.1016/j.jpowsour.2010.04.027

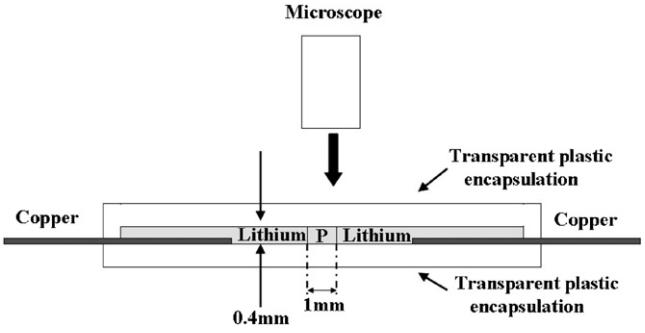

Fig. 1. Schematic presentation of assembly of the optically visible test cell.

electrolyte was reported. The Li/PEO–LiTFSI/Li cell showed dendrite growth at 0.6 h with a polarization of 0.7 mA cm^{-2}, where the separator was approximately 1 mm thick [11]. The lithium dendrite growth is dependent on the current density. Dendrite formation of the same cell configuration started at 42 h for a polarization of 0.05 mA cm^{-2} [12]. For practical applications, the dendrite formation onset time should be more prolonged at higher current density.

In this study, the dendrite formation in Li/PEO–LiTFSI/Li has been examined by direct *in situ* observation, and the effect of the addition of nano-SiO_2 and acid-modified nano-SiO_2 into PEO–LiTFSI on the lithium dendrite growth is described as a function of the current density. The relationship between lithium dendrite formation and the Li/polymer electrolyte interfacial resistance is also discussed.

2. Experimental

The PEO–LiTFSI–SiO_2 composite polymer electrolyte was prepared using a previously reported casting technique [13]. PEO powder (Aldrich, average molecular weight of 6×10^5) and LiTFSI (Fluka, Li/O = 1/18) were completely dissolved in anhydrous acetonitrile (AN). SiO_2 (Kanto Chemicals, 50 nm average particle size) was dried at 200 °C for 24 h under vacuum. The acid-modified nano-SiO_2 was obtained by impregnating the SiO_2 particles with 0.1 M H_2SO_4 solution for 10 h at room temperature, drying at 100 °C in air and then at 200 °C under vacuum for 24 h, followed by milling of the SiO_2 particles for 2 h using a high speed planetary ball mill. The nano-SiO_2 or the acid-modified nano-SiO_2 was homogeneously dispersed in the PEO-LiTFSI solution as a filler (10 wt%) by stirring

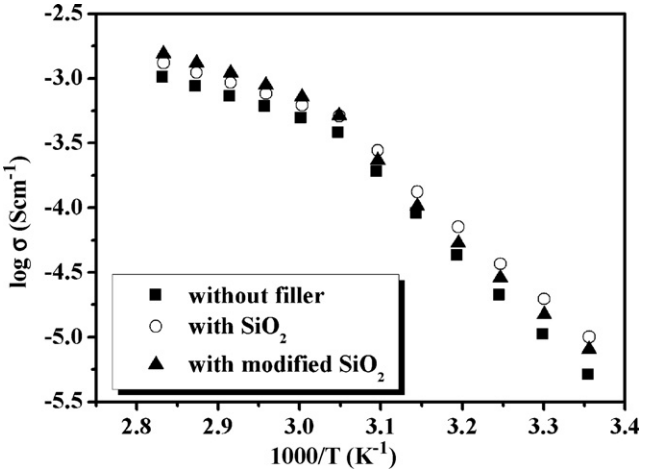

Fig. 2. Temperature dependence of the electrical conductivity of PEO_{18}LiTFSI, PEO_{18}LiTFSI–10 wt% nano-SiO_2, and PEO_{18}LiTFSI–10 wt% acid-modified nano-SiO_2.

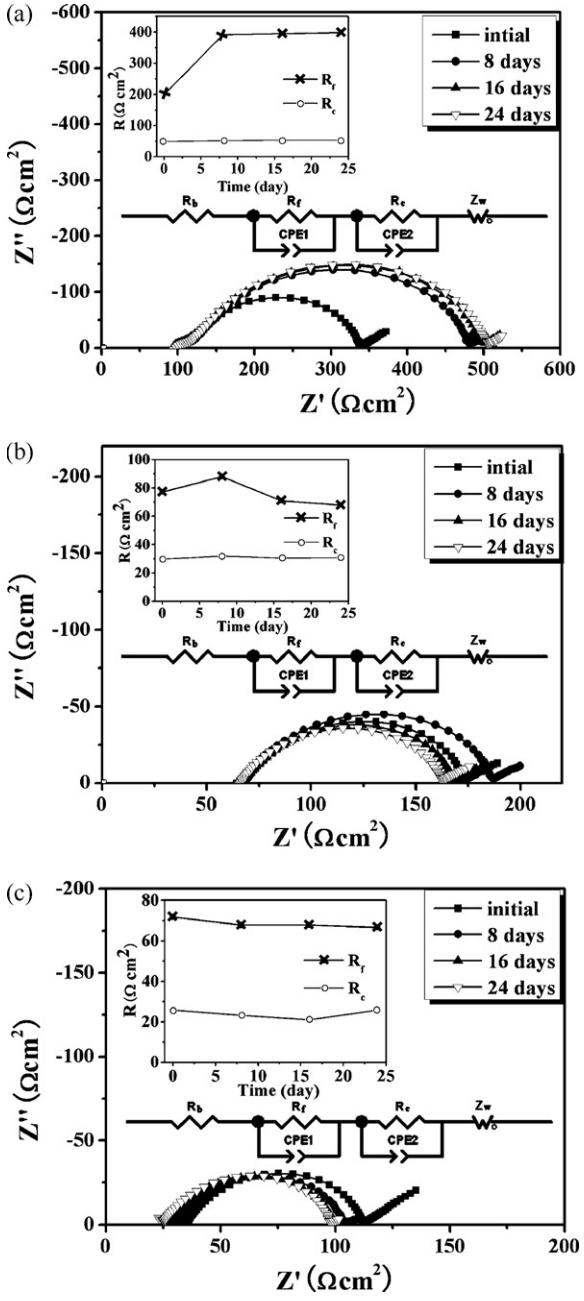

Fig. 3. Impedance spectra of Li/PEO_{18}LiTFSI/Li (a), Li/PEO_{18}LiTFSI–10 wt% nano-SiO_2/Li (b), and Li/PEO_{18}LiTFSI–10 wt% acid-modified nano-SiO_2 (c) at 60 °C as a function of the storage time. The inset figures show changes of R_f and R_c values with storage time.

at room temperature for 24 h in an Ar-filled dry glove box and the mixture was then cast into a clean Teflon dish. The AN solvent was evaporated slowly at 40 °C in a dry Ar atmosphere for 12 h and then dried at 110 °C for 12 h under vacuum. The polymer electrolyte was obtained as homogeneous films with an average thickness of 230 μm.

Two types of cells, a sandwich cell and a visualization cell, were used. A sandwich cell of Au/PEO_{18}LiTFSI–SiO_2/Au was used for electrical conductivity measurements and a Li/PEO_{18}LiTFSI–SiO_2/Li cell was used for interface resistance and electrochemical experiments. The visualization cell was used for the *in situ* examination of the formation and evolution of dendrites. Two narrow lithium metal strips (0.4 mm wide) with copper film leads were placed end to end on the polymer electrolyte with a distance of ca. 1 mm between the two

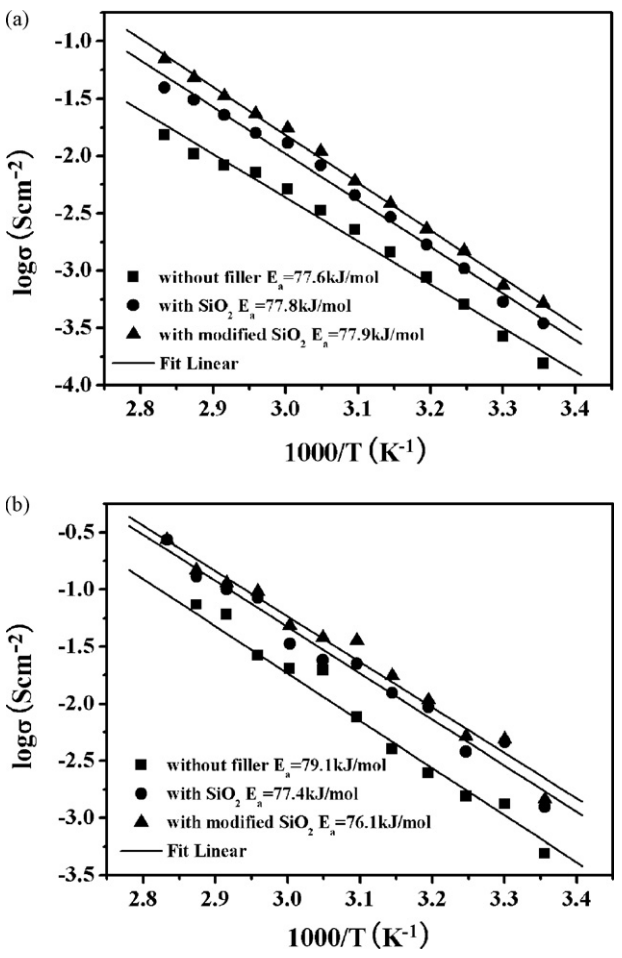

Fig. 4. Temperature dependence of the inverse of the specific surface interface resistance (R_f) (a) and the inverse of the specific charge transfer resistance (R_c) (b) of Li/PEO_{18}LiTFSI/Li (■), Li/PEO_{18}LiTFSI–10 wt% nano-SiO_2/Li (●), and Li/PEO_{18}LiTFSI–10 wt% acid-modified nano-SiO_2 (▲).

electrodes. The cell was sandwiched between two pieces of a plastic film with low water and gas permeability. The plastic film envelope was then evacuated and heat-sealed. Fig. 1 shows the experimental set-up of the visualization cell. Dendrite growth was observed *in situ* using a digital microscope (VHX-100, Keyence).

Electrochemical impedance spectroscopy (EIS) measurements were conducted using a frequency response analyzer (Solartron 1260) with an electrochemical interface (Solartron 1287) in the frequency range from 1 MHz to 0.01 Hz.

3. Results and discussion

The addition of nanosize fillers such as SiO_2, TiO_2 and Al_2O_3 to PEO-based lithium conducting polymer electrolytes has induced improvement in the transport properties [14]. Scrosati et al. [14] reported that the presence of nano-SiO_2 in $PEO_{30}LiClO_4$ enhanced the electrical conductivity by approximately two orders of magnitude from 10^{-7} to 10^{-5} S cm^{-1} at room temperature and reduced the resistance of the Li/$PEO_{30}LiClO_4$–SiO_2/Li cell. Fig. 2 shows Arrhenius plots for the electrical conductivity of PEO_{18}LiTFSI with and without nano-SiO_2 filler for a Au/PEO_{18}LiTFSI–SiO_2/Au cell. The conductivity enhancement by addition of nano-SiO_2 to PEO_{18}LiTFSI is not significant, but the room temperature conductivity of PEO_{18}LiTFSI (ca. 10^{-5} S cm^{-1}) is comparable to that of $PEO_{30}LiClO_4$ with nano-SiO_2. The activation energies for conduction in PEO_{18}LiTFSI with and without the SiO_2 filler are similar,

Table 1
Change of R_f and R_c values with storage time.

PEO_{18}LiTFSI	R (Ω cm^2)	Initial	8 days	16 days	24 days
Without filler	R_f	199.1	391.5	395.2	398.7
	R_c	49.4	52.0	53.7	53.0
With SiO_2	R_f	77.2	87.9	71.0	67.8
	R_c	29.8	31.9	30.6	30.8
With acid-modified SiO_2	R_f	71.8	67.8	67.8	66.6
	R_c	25.7	23.3	21.1	25.8

because the conductivity enhancement by addition of the SiO_2 filler is not significant for a high conductivity polymer electrolyte system with a high segmental motion of polymer chains.

As previously reported [14,15], the interface resistance between a lithium metal electrode and polymer electrolyte increases with the contact period and is reduced by the addition of fillers. The interface resistance dominates the cell resistance of the Li/polymer electrolyte/Li cell. Fig. 3 shows the time dependence of the typical impedance responses for Li/PEO_{18}LiTFSI/Li symmetric cells with nano-SiO_2, acid-modified nano-SiO_2 and without filler at 60 °C. These impedance spectra show a small semi-circle in the high frequency range and a large slightly depressed semicircle in the mid frequency range, followed by a spur inclined at approximately 45°, which is typical of the diffusion phenomenon of ions. The small semicircle in the high frequency range could be assigned as the grain boundary resistance of PEO_{18}LiTFSI (R_g), because a similar

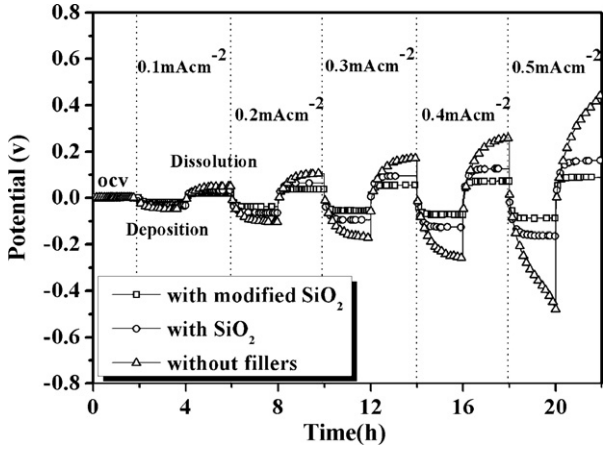

Fig. 5. Constant current polarization curves in Li/PEO_{18}LiTFSI/Li with and without the nano-SiO_2 filler at 60 °C.

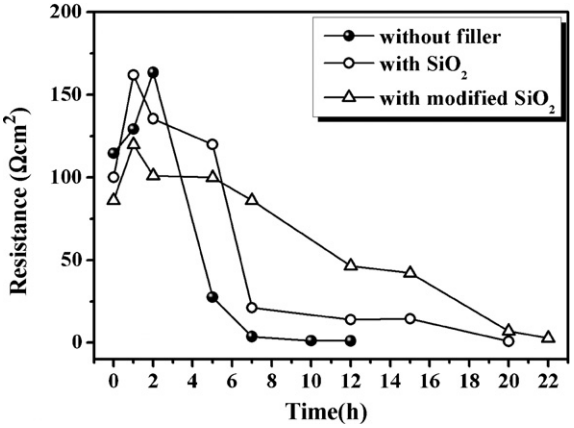

Fig. 6. Li/PEO_{18}LiTFSI–nano-SiO_2/Li cell resistance change with time at 0.5 mA cm^{-2} and at 60 °C.

small semicircle was observed in the same frequency range for the Au/PEO_{18}LiTFSI/Au cell. All the spectra include a resistance at the high frequency intercept of the semi-circle with the real axis, which can be ascribed to the bulk resistance (R_b) of the polymer electrolyte. The diameter of the large semicircle is associated with the overall interfacial resistance (R_i), which consists of two parts, the resistance of the passivation film (R_f) formed on the lithium electrode surface by reaction with the polymer electrolyte and the charge-transfer resistance (R_c) of the $Li^+ + e^- = Li$ reaction [15]. The impedance spectra were subjected to a nonlinear least-squares fit program to obtain the impedance parameters using the equivalent circuit shown in Fig. 3. Analysis of the impedance spectra for Li/PEO_{18}LiTFSI/Li at 60 °C after a few hours contact of the lithium metal and the polymer electrolyte yielded $R_b = 110\ \Omega\,cm^2$, $R_f = 199\ \Omega\,cm^2$, and $R_c = 50\ \Omega\,cm^2$. R_f and R_c increased during the first 7 days of storage and then stable resistances of $R_f = 293\ \Omega\,cm^2$ and $R_c = 112.6\ \Omega\,cm^2$ were observed during 24 days of storage at 60 °C. R_b is almost constant over the 24 days of storage and is comparable to the resistance measured with the Au/PEO_{18}LiTFSI/Au cell. The PEO_{18}LiTFSI electrolyte with the nano-SiO_2 filler showed low and stable interfacial resistances. The R_f of 74 $\Omega\,cm^2$ decreased to 59 $\Omega\,cm^2$ and the R_c of 28 $\Omega\,cm^2$ increased to 39.6 $\Omega\,cm^2$ after 24 days of storage at 60 °C. The sum of R_f and R_c was almost unchanged after storage, so that these small changes may be included within the deviation of the fitting results. The stable interface resistances are less than one fourth of those without the filler. Furthermore, the Li/PEO_{18}LiTFSI/Li cell with acid-modified nano-SiO_2 had a more stable and lower interfacial resistance. The initial R_f of 57 $\Omega\,cm^2$ decreased to 42.1 $\Omega\,cm^2$ and the R_c of 20 $\Omega\,cm^2$ slightly increased to 32.2 $\Omega\,cm^2$ after 24 days of storage at 60 °C. R_c and R_f of the Li/PEO_{18}LiTFSI/Li cell with the acid-modified SiO_2 decreased more than those with the pristine nano-SiO_2. The calculated R_f and R_c values with storage time are summarized in Table 1. Sannier et al. reported that some fillers with superacid surface groups have a positive effect on the interfacial stability of the lithium electrode–polymer electrolyte interface [16]. According to this concept, introduction of superacidic groups onto the acid-modified nano-SiO_2 surface immobilizes basic species (PEO chain and anions) and promotes the movement of lithium ions also. In addition, the Lewis acid surface of the acid-modified nano-SiO_2 scavenges any trace water in the polymer electrolyte, thereby preventing reaction of the trace water with lithium metal. Fig. 4 shows Arrhenius plots of the inverse (a) surface passivation film resistance of R_f and (b) charge transfer resistance of R_c. These curves show no knee in the temperature range examined. The activation energies for the passivation layer and the charge transfer at the interface of the lithium metal and passivation layer are almost the same at approximately 78 and 77 kJ mol^{-1}, respectively. In addition, these values are almost independent of the presence or absence of the filler. R_f is higher than R_c in the observed temperature range. The activation energy for the electrical conductivity of the passivation layer is higher than that for the electrical conductivity

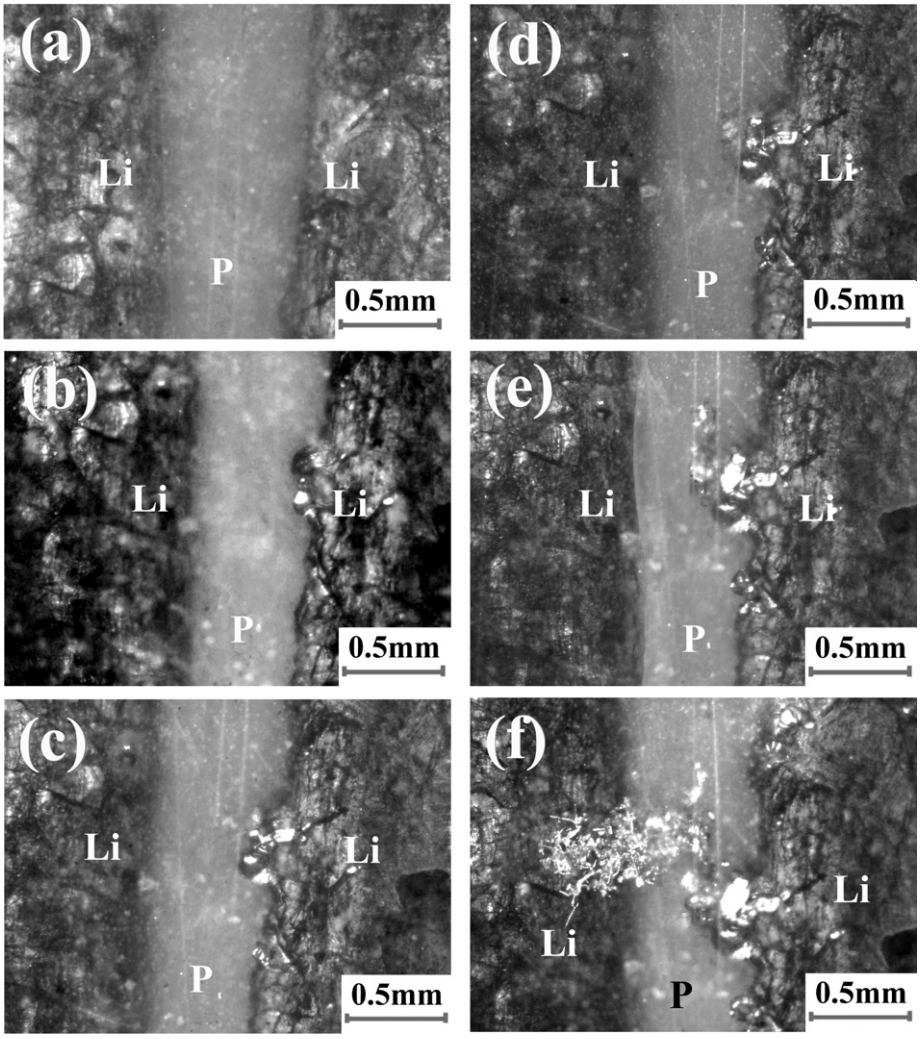

Fig. 7. Dendrite growth in a visualization Li/PEO_{18}LiTFSI/Li cell at 60 °C and 0.1 mA cm^{-2} at (a) $t = 0$ h, (b) $t = 125$ h, (c) $t = 135$ h, (d) $t = 155$ h, (e) $t = 185$ h, and (f) $t = 225$ h.

of PEO_{18}LiTFSI (ca. 38 kJ mol^{-1}). It is not currently clear as to the type of passivation layer that is formed between lithium metal and PEO_{18}LiTFSI. The passivation layer resistance is dominant in the cell resistance of Li/PEO_{18}LiTFSI/Li and the addition of acid-modified nano-SiO_2 to PEO_{18}LiTFSI is quite effective to reduce this resistance.

The polarization potentials of the Li/PEO_{18}LiTFSI/Li cell were measured as a function of the current density for the Li/PEO_{18}LiTFSI/Li cell with and without SiO_2 filler. Fig. 5 shows the results in the current density range of 0.1–0.5 mA cm^{-2} at 60 °C. At high current densities, the cell without the filler exhibits high polarization potentials with increasing time, while the cell with the acid-modified nano-SiO_2 filler shows the lowest stable polarization potentials with time. The improvement of the electrochemical performance could be ascribed to the decrease in the interfacial resistance by addition of the acid-modified nano-SiO_2 filler. The cell resistance changes with time for the sandwich Li/PEO_{18}LiTFSI/Li cells both with and without the nano-SiO_2 filler at 60 °C and at current density of 0.5 mA cm^{-2}, as shown in Fig. 6, where the lithium electrode thickness was approximately 230 μm. All cells displayed an increase in cell resistance during the initial stage, which then decreased over time to zero. Zero cell resistance indicates short circuit caused by dendrite growth; therefore, the decrease in cell resistance can be explained by lithium dendrite formation. The onset time for decrease of the cell resistance and the short circuit time are extended by addition of the nano-SiO_2 filler into PEO_{18}LiTFSI, which suggests the suppression of dendrite formation by addition of the nano-SiO_2 filler.

To confirm the onset and growth of dendrite formation, visualization cells (Fig. 1) were used to observe the lithium electrode/electrolyte interface after polarization at different current densities and at 60 °C. Note that the geometry of the visualization cell is very different from that of the sandwich cell. The short circuit time (t_s) in the visualization cells was expected to be much longer than that in the sandwich cell, because the distance between the electrodes is much larger; however, the effect of filler addition into PEO_{18}LiTFSI could be easily observed. Figs. 7 and 8 show typical dendrite growth in the Li/PEO_{18}LiTFSI/Li visualization cells at current densities of 0.1 and 0.5 mA cm^{-2}, respectively. The dendrite formation onset time is dependent on the polarization current density; therefore, at a lower current density of 0.1 mA cm^{-2}, dendrite formation is observed after 125 h polarization and after 15 h polarization at the higher current density of 0.5 mA cm^{-2}. Brissot et al. [11] reported similar results using a Li/PEO_{20}LiTFSI/Li visualization cell at 0.05 mA cm^{-2} and at 80 °C, where the distance between the two lithium electrodes was approximately 1 mm as in our cells. Dendrite formation was observed after 38 h polarization and the largest dendrite contacted the opposing electrode after 100 h polarization. The onset times of the dendrite formation from our results are longer than those reported by Brissot et al. Dendrite formation is also dependent on the surface morphology of the lithium metal and the polymer electrolyte, and the water content in the electrolyte, in addition to the current density, as shown in Figs. 7 and 8. At lower current density, more lithium metal can be deposited on lithium metal without dendrite formation (3.23 mg cm^{-2} at 0.1 mA cm^{-2} and 1.94 mg cm^{-2} at 0.5 mA cm^{-2}). Figs. 9 and 10 show the dendrite growth in the Li/PEO_{18}LiTFSI–10 wt% nano-SiO_2/Li and Li/PEO_{18}LiTFSI–10 wt% acid-modified SiO_2/Li visualization cells at 60 °C and at a current density of 0.5 mA cm^{-2}, respectively. The results show the onset times of dendrite formation are prolonged by addition of the SiO_2 filler into PEO_{18}LiTFSI, and especially for the addition of the acid-modified nano-SiO_2; the onset time of dendrite formation at the Li/PEO_{18}LiTFSI interface at 0.5 mA cm^{-2} at 60 °C of 15 h was extended to 32 h by addition of 10 wt% acid-modified nano-SiO_2 into PEO_{18}LiTFSI. The suppression of dendrite formation could be explained by the low interfacial resistance between lithium metal and PEO_{18}LiTFSI with addition of acid-modified nano-SiO_2. Brissot et al. [11] observed that at high current density the dendrites started to form when the ionic concentration dropped to zero at the negative electrode, whereas at low current density, local inhomogeneities seem to play a major role. The polarization potentials of Li/PEO_{18}LiTFSI/Li at higher current density were significantly reduced by addition of acid-modified nano-SiO_2 (Fig. 6), that is, the lithium ion concentration at the negative electrode was maintained for a long period. The short circuit of the Li/PEO_{18}LiTFSI–10 wt% acid-modified SiO_2/Li cell at 0.5 mA cm^{-2} and at 60 °C was observed after 42 h polarization, which is longer than that observed in the sandwich cell shown in Fig. 6.

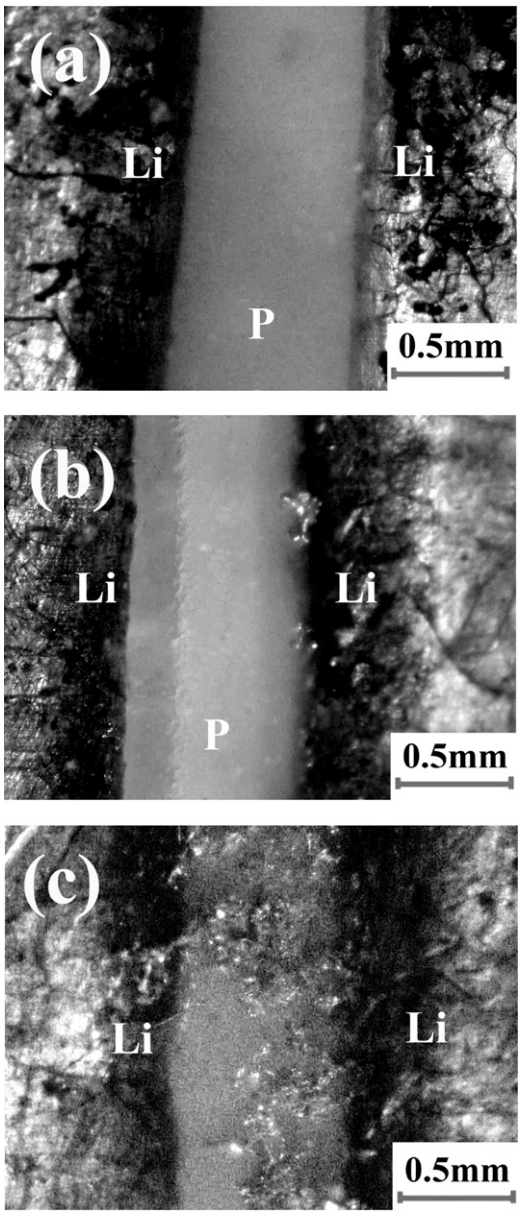

Fig. 8. Dendrite growth in a visualization Li/PEO_{18}LiTFS/Li cell at 60 °C and 0.5 mA cm^{-2} at (a) t = 0 h, (b) t = 15 h, and (c) t = 20 h.

Table 2 summarizes the onset time of the dendrite formation and short circuit with different current densities for the Li/PEO_{18}LiTFSI/Li cells with and without the nano-SiO_2 filler at 60 °C. Rosso et al. [12] observed that the onset time of dendrite formation followed a power law as a function of the current density (i) that was very close to Sand's law [17] in the current density range from 0.02 to 0.3 mA cm^{-1}; the time to a partial short

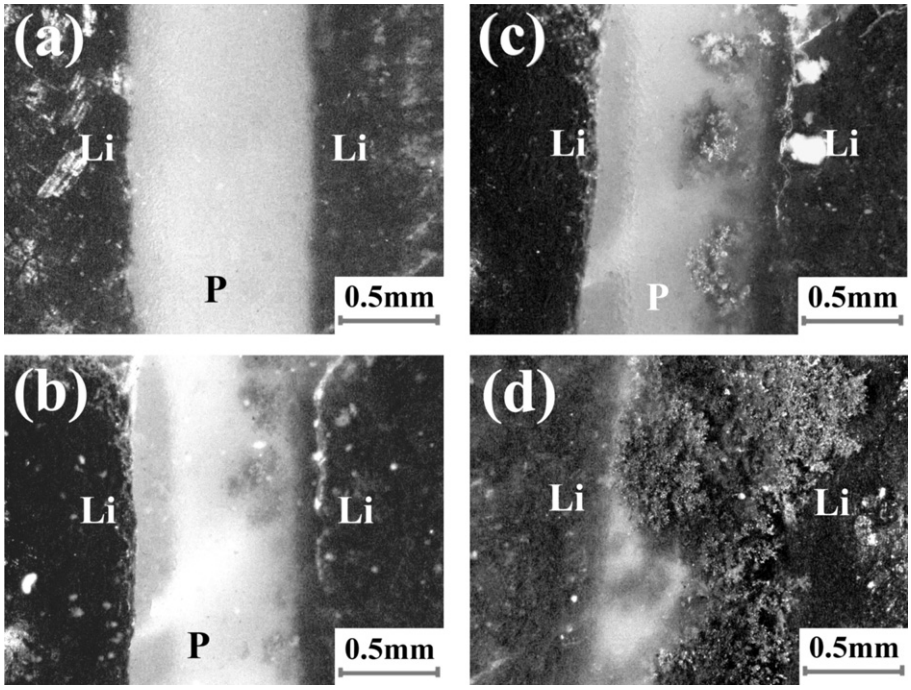

Fig. 9. Dendrite growth in a visualization Li/PEO_{18}LiTFSI–10 wt% nano-SiO_2/Li cell at 60 °C and 0.5 mA cm^{-2} at (a) t = 0 h, (b) t = 25 h, (c) t = 30 h, and (d) t = 40 h.

circuit of the cell by dendrite formation followed a i^{-2} dependence. However, our results in the current range from 0.1 to 1.0 mA cm^{-2} were far from the results reported by Rosso et al. [12], as shown in Fig. 11, where the slope of the $\ln t_s$ vs. $\ln J$ is approximately −1.3. Therefore, the dendrite formation at high current density does not obey Sand's law, because the non-uniformity of the lithium–electrolyte interface may play a more important role [12,18]. The short circuit time in the Li/PEO_{18}LiTFSI–acid-modified nano-SiO_2/Li cell of 20 h at 60 °C is compared with that of the Li/ethylene carbonate–dimethyl carbonate–ethyl methyl carbonate (1:1:1)–$LiPF_6$/Li, where short circuit by dendrite formation was observed after 0.2 h polarization at 1 mA cm^{-2} and at 35 °C. For the practical application of a water stable Li electrode/polymer electrolyte/water-stable lithium-conducting solid electrolyte for high energy density lithium–air batteries, the lithium anode should be dendrite free at high current drain. The Li/PEO_{18}LiTFSI–10 wt%

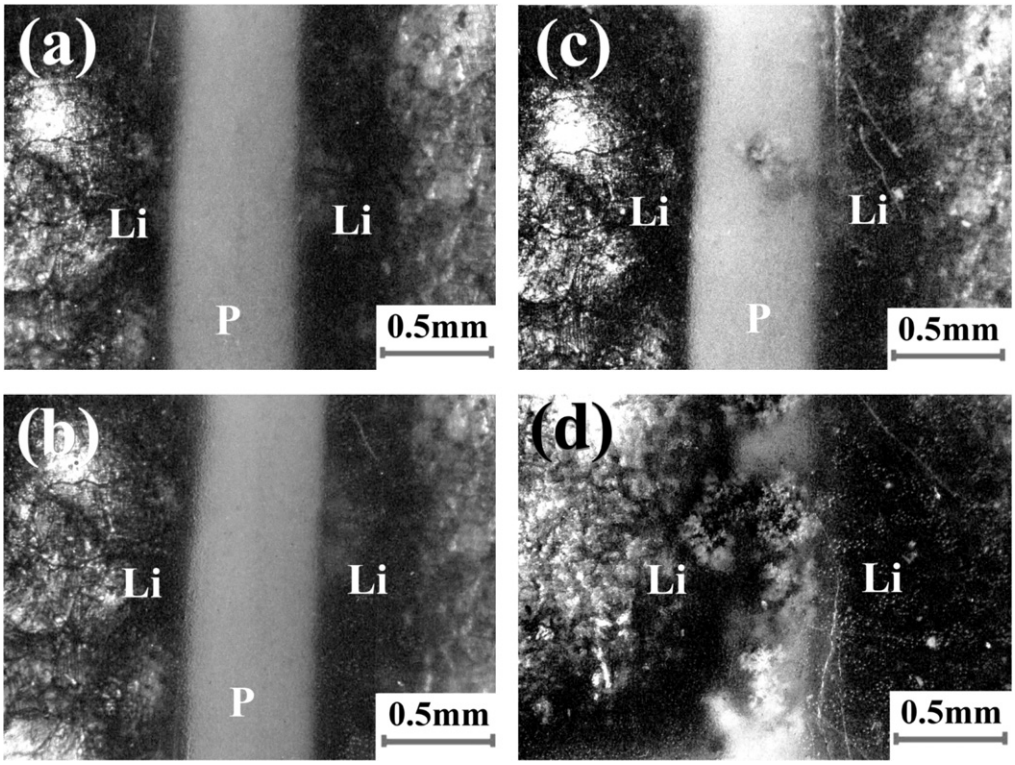

Fig. 10. Dendrite growth in a visualization Li/PEO_{18}LiTFSI–10 wt% acid-modified nano-SiO_2/Li cell at 60 °C and 0.5 mA cm^{-2} at (a) t = 0 h, (b) t = 25 h, (c) t = 32 h, and (d) t = 42 h.

Table 2
Onset (t_o) and short-circuit (t_s) times for lithium dendrite formation.

PEO_{18}LiTFSI	Current density (mA cm^{-2})	t_o (h)	t_s (h)
Without filler	0.1	125	225
	0.25	60	76
	0.5	15	20
	1.0	10	15
With SiO_2	0.1	205	355
	0.25	70	90
	0.5	25	40
	1.0	10–15	15
With acid-modified SiO_2	0.1	250	400
	0.25	96	114
	0.5	32	42
	1.0	15–20	20

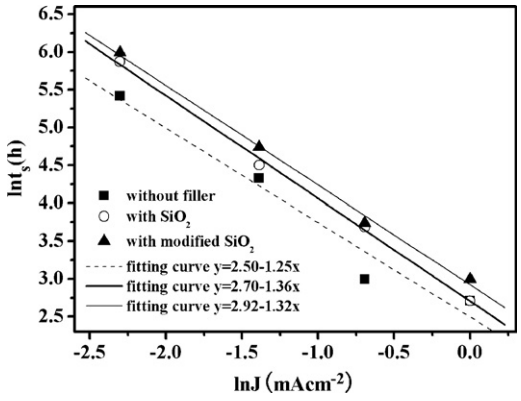

Fig. 11. Variation of the short-circuit time (t_s) as a function of the current density (J) at 60 °C for visualization cells of Li/PEO_{18}LiTFSI/Li with and without the nano-SiO_2 filler.

acid-modified SiO_2/Li cell showed dendrite formation after 32 h under polarization at 0.5 mA cm^{-2} and at 60 °C. The capacity of 16 mAh cm^{-2} corresponds to 4.1 mg cm^{-2} of Li metal. Generally, the Li metal anode is used with a copper substrate sheet; therefore, the total weight of the lithium anode (4.1 mg cm^{-2}) with a 10 μm thick copper substrate becomes 13.7 mg cm^{-2}, the capacity of which is 1170 mAh g^{-1}. This specific capacity is almost 30% that of lithium metal, but more than three times higher than that of graphite.

4. Conclusion

The interfacial resistance of Li/PEO_{18}LiTFSI/Li was significantly reduced by the addition of nano-SiO_2 and acid-modified nano-SiO_2 fillers to the PEO_{18}LiTFSI polymer electrolyte, and the electrical conductivity of PEO_{18}LiTFSI was slightly increased. In particular, the acid-modified nano-SiO_2 was effective to reduce the interfacial resistance. Lithium dendrite growth was observed using a visualization cell, which showed that dendrite growth was effectively prevented by the introduction of the acid-modified nano-SiO_2 filler into PEO_{18}LiTFSI. The short circuit period of 225 h for the Li/PEO_{18}LiTFSI/Li cell at 0.1 mA cm^{-2} and at 60 °C was extended to 400 h by addition of the acid-modified nano-SiO_2. The period until short circuit by dendrite formation was dependent on the current density; at 0.5 mA cm^{-2}, short circuit was observed at 42 h. The estimated specific capacity of a lithium electrode with a 10 μm thick Cu substrate until short circuit in Li/PEO_{18}LiTFSI/Li was 1170 mAh g^{-1} at 0.5 mA cm^{-2} and at 60 °C. A water-stable lithium anode with PEO_{18}LiTFSI–10 wt% acid-modified nano-SiO_2 and a water-stable lithium-conducting solid electrolyte could be used as the lithium electrode for high energy density lithium–air secondary batteries. However, the development of a lithium–polymer electrolyte system without lithium dendrite formation at higher current density is required.

Acknowledgements

This work was supported by the New Energy and Industrial Technology Development Organization (NEDO) of Japan under the “Development of High Performance Battery System for Next-Generation Vehicles” project.

References

[1] E. Peled, J. Electrochem. Soc. 126 (1979) 2047.
[2] C. Brissot, M. Rosso, J.-N. Chazalviel, P. Baudry, S. Lascaud, Electrochim. Acta 43 (1998) 1569.
[3] S. Megahed, B. Scrosati, Interface 4 (4) (1995) 34.
[4] W.H. Meyer, Adv. Mater. 10 (1998) 439.
[5] M. Armand, J.-M. Tarascon, Nature 451 (2008) 652.
[6] S.J. Visco, E. Nimon, B. Katz, L.D. Jonghe, M.-Y. Chu, The 210th Electrochem. Soc. Meeting Abstracts #389, 2006.
[7] T. Zhang, N. Imanishi, S. Hasegawa, A. Hirano, J. Xie, Y. Takeda, O. Yamamoto, N. Sammes, Electrochem. Solid-State Lett. 12 (2009) A132.
[8] T. Zhang, N. Imanishi, S. Hasegawa, A. Hirano, J. Xie, Y. Takeda, O. Yamamoto, N. Sammes, J. Electrochem. Soc. 155 (2008) A965.
[9] H.E. Park, C.H. Hong, W.Y. Yoon, J. Power Sources 178 (2008) 765.
[10] T. Matsui, K. Takeyama, Electrochim. Acta 40 (1995) 2165.
[11] C. Brissot, M. Rosso, J.-N. Chazalviel, S. Lascaud, J. Power Sources 81–82 (1999) 925.
[12] M. Rosso, T. Gobron, C. Brissot, J.-N. Chazalviel, S. Lascaud, J. Power Sources 97–98 (2001) 804.
[13] Y. Liu, Y. Takeda, T. Matsumura, J. Yang, N. Imanishi, A. Hirano, O. Yamamoto, J. Electrochem. Soc. 153 (2006) A437.
[14] B. Scrosati, F. Croce, L. Persi, J. Electrochem. Soc. 147 (2000) 1718.
[15] G.B. Appetecchi, F. Croce, G. Doutzenberg, M. Mastragostino, F. Ronci, B. Scrosati, F. Soavi, A. Zanelli, F. Alessandrini, P.P. Prosini, J. Electrochem. Soc. 145 (1998) 4126.
[16] L. Sannier, A. Zalewska, W. Wieczorek, M. Marczewski, H. Marczewska, Electrochim. Acta 52 (2007) 5685.
[17] H.J.S. Sand, Philos. Mag. Ser. 6 (1) (1901) 45.
[18] M. Rosso, E. Chassaing, J.N. Chazalviel, T. Gobron, Electrochim. Acta 47 (2002) 1267.